JACS
JOURNAL OF THE AMERICAN CHEMICAL SOCIETY
Communication
pubs.acs.org/JACS

Oxidation of Highly Unstable <4 nm Diameter Gold Nanoparticles 850 mV Negative of the Bulk Oxidation Potential

Rafael A. Masitas and Francis P. Zamborini*

Department of Chemistry, University of Louisville, Louisville, Kentucky 40292, United States

Supporting Information

ABSTRACT: Here we describe the oxidation of <4 nm diameter Au nanoparticles (NPs) attached to indium tin oxide-coated glass electrodes in Br^- and Cl^- solution. Borohydride reduction of $AuCl_4^-$ in the presence of hexanethiol or trisodium citrate (15 min) led to Au NPs <4 nm in diameter. After electrochemical and ozone removal of the hexanthiolate ligands from the thiol-coated Au NPs, Au oxidation peaks appeared in the range 0−400 mV vs Ag/AgCl (1 M KCl), which is 850−450 mV negative of the bulk Au oxidation peak near 850 mV. The oxidation potential of citrate-coated Au NPs is in the 300−500 mV range and those of 4 and 12 nm diameter Au NPs in the 660−780 mV range. The large negative shift in potential agrees with theory for NPs in the 1−2 nm diameter range. The oxidation potential of Au in Cl^- solution is positive of that in Br^- solution, but the difference decreases dramatically as the NP size decreases, showing less dependence on the halide for smaller NPs.

Metal nanoparticles (NPs) exhibit fascinating size-dependent properties that are useful for a wide range of applications. Smaller-sized NPs are often the most effective for certain applications, especially in catalysis, sensing, and nanoelectronics, due to their high surface area and dramatic change in their electronic structure. Small NPs of Au and Ag have exhibited fluorescence,[1] and there has been a recent heightened awareness about the toxicity of metallic NPs, which is often attributed to the liberation of metal ions.[2] Thus, the stability of metal NPs against oxidation is a crucial issue.

Previously, on the basis of sublimation energies, Henglein predicted a large negative shift in the oxidation potential of small Ag clusters of a few atoms and showed that such clusters behave as strong reducing agents.[3] On the basis of the increase in surface area, Plieth predicted a $1/r$-dependent negative shift in the oxidation potential relative to the bulk metal for metal NPs with radius r.[4] Recently, Sieradzki and co-workers showed that <4 nm diameter Pt NPs dissolve at potentials well below the bulk value and by a different mechanism.[5a] They developed size-dependent potential−pH diagrams and imaged dissolving Pt NPs by scanning tunneling microscopy (STM).[5b] Del Popolo et al.[6] reported that small Pd NPs dissolve at more negative oxidation potentials relative to the bulk, while Kolb[7] and Penner[8] showed an enhanced stability of Cu and Ag NPs on Au and highly ordered pyrolitic graphite, respectively, by STM. Compton and co-workers observed no change in the oxidation potential for Ag NPs over the 25−100 nm diameter range.[9] Brus and co-workers described an electrochemical Ostwald ripening process for Ag on conductive substrates that was due to the more negative oxidation potential for smaller NPs.[10] Recently, Brainina and co-workers described the size-dependent oxidation of metal NPs theoretically[11a] and later compared theory to experimental data for the oxidation of Au in chloride solution.[11b]

Our group was the first to quantify the negative shift in the oxidation potential of Ag (8−50 nm diameter)[12a] and Au (4 to 250 nm diameter)[12b] NPs as a function of size directly by voltammetry and compare the results to the theory developed by Plieth.[4] The agreement was better for Au, which showed an ∼200 mV negative shift in potential between bulk Au (≥60 nm) and 4 nm diameter NPs. On the basis of the expected $1/r$ dependence, the negative shift should increase dramatically for sizes below 4 nm, which is the focus of this work.

We synthesized <4 nm diameter hexanethiolate (C6S)-coated Au monolayer-protected clusters (MPCs)[13] or citrate-protected Au NPs[12] in solution, chemically attached them to functionalized glass/indium tin oxide (ITO) electrodes, and studied the electrochemical oxidation by linear sweep voltammetry (LSV) in a similar manner as described in our previous studies.[12] [All experimental details are in the Supporting Information (SI).] Figure 1A shows the results of the oxidation of 2.5 ± 0.7 nm average diameter C6S Au MPCs (blue plot) on a thiol-functionalized glass/ITO electrode. The size was based on transmission electron microscopy (TEM) images, which showed NP diameters ranging from 1 to 5 nm, with ∼79% of the NPs below 3 nm and 21% above 3 nm (Figure S1 in the SI). After attachment to the electrode, we removed the C6S ligands electrochemically and with ozone (Figure S2). The LSV showed a large oxidation peak near 720 mV along with four smaller oxidation peaks in the 0−400 mV range. Au can be oxidized in the presence of halides by the following reactions:[14]

$$Au^0 + 4Br^- \rightarrow AuBr_4^- + 3e^- \quad E^\circ = 0.85\ V\ (0.99\ V\ for\ Cl^-)$$

$$Au^0 + 2Br^- \rightarrow AuBr_2^- + e^- \quad E^\circ = 0.96\ V\ (1.15\ V\ for\ Cl^-)$$

$$2Au^0 + AuBr_4^- + 2Br^- \rightarrow 3AuBr_2^- \quad (chemical)$$

The three-electron (3e) oxidation is thermodynamically favorable, but our group previously reported an average oxidation of 1.5 electrons, while others reported 1.9 electrons.[14] This could be due to a combination of the direct 3e and one-

Received: November 19, 2011
Published: February 28, 2012

   dx.doi.org/10.1021/ja2108933 | J. Am. Chem. Soc. 2012, 134, 5014−5017

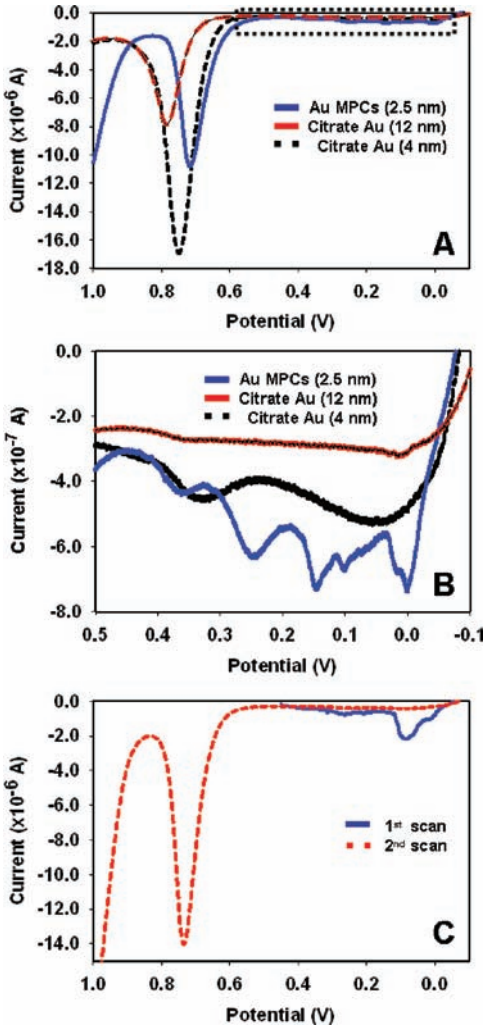

Figure 1. (A) LSVs for Au NPs with diameters of 2.5 nm (blue solid plot), 4.0 nm (black dashed plot), and 12 nm (red dashed plot) in 0.1 M $HClO_4$ + 0.01 M KBr from −0.1 to 1.0 V. (B) Expanded view of the region from −0.1 to 0.5 V, marked by the dotted box in (A). (C) LSV of 2.5 nm diameter Au MPCs from −0.10 to 0.45 V (first scan) and −0.1 to 1.0 V (second scan).

electron (1e) oxidations or the third chemical step shown above. While the situation is quite complex, we previously observed one main peak for the oxidation of Au NPs from 4 to 250 nm in diameter.[12b] Accordingly, we attribute the distinct peaks in the LSV in Figure 1 to different Au NP sizes as opposed to the different reactions above. The red and black dashed plots, respectively, show the oxidations of well-characterized 12 and 4 nm average diameter citrate-coated Au NPs attached to amine-functionalized glass/ITO for comparison. Figure 1B shows an expanded view of the LSV from −100 to 500 mV. The peaks are somewhat symmetrical and consistent with surface oxidative stripping. No peaks exist in the low potential range for the larger 12 nm diameter Au NPs, and two broad, weakly defined peaks exist for the 4 nm diameter sample. On the basis of the three plots, we attribute the peak at 720 mV for the Au MPC sample to the oxidation of Au NPs near 4.0 nm in diameter and those from 0 to 400 mV to the oxidation of <4.0 nm diameter Au NPs.

Figure 1C shows an experiment where we attached the 2.5 nm average diameter Au NPs onto the electrode and performed the first scan from −0.1 to 0.45 V and a second scan from −0.1 to 1.0 V. The first scan showed a noticeable oxidation peak near 100 mV, which we attribute to the oxidation of <4.0 nm diameter Au NPs. In the second scan, this peak was absent, and we observed only an oxidation peak near 740 mV. The absence of a peak in the 0−400 mV range in the second scan is consistent with removal of the Au NPs by oxidative dissolution, whereby the Au dissolved and diffused away from the electrode. The peak at 740 mV correlates with the oxidation of 4 nm diameter Au NPs that did not oxidize in the first scan because the potential was not positive enough.

Figure 2 shows the LSV of 2.5 nm average diameter Au MPCs on thiol-functionalized glass/ITO in 0.1 M $HClO_4$ +

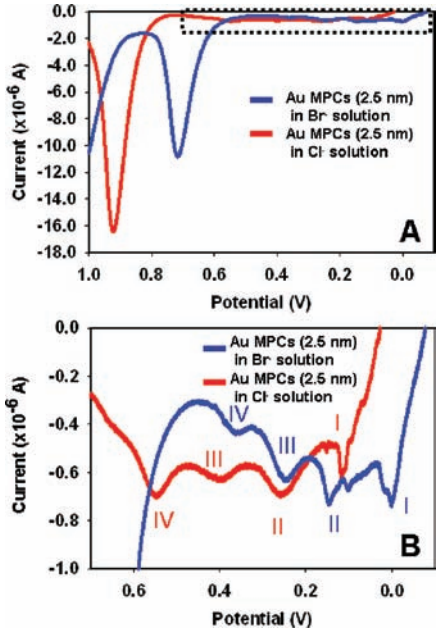

Figure 2. (A) LSVs of 2.5 nm average diameter Au MPCs in 0.1 M $HClO_4$ plus 0.01 M KBr (blue plot) or 0.01 M KCl (red plot). (B) Expanded view of the region from −0.1 to 0.7 V (dotted box in A).

0.01 M Cl^- solution (red curve) compared with 0.01 M Br^- (blue curve). The peak at 720 mV in Br^- shifted to ∼940 mV in Cl^-, and the four lower oxidation peaks shifted in the positive direction to the 110−550 mV range. The oxidation of Au in Cl^- solution occurs by the reactions shown above with Br^- replaced by Cl^-, at potentials ∼140 mV and 19 mV more positive than the values for Br^- for the 3e and 1e oxidations, respectively, since Cl^- coordinates more weakly with Au than Br^- does. We observed the same peaks in both LSVs, but the peaks were shifted in the positive direction in Cl^-, consistent with Au metal oxidation by the halides. The shift in the oxidation of the 4 nm diameter NPs (∼220 mV) is larger than expected for the 3e process and much larger than expected for the 1e process. The shift in the oxidation of the smaller <4 nm diameter Au NPs (∼110−180 mV) decreased with decreasing oxidation potential (or smaller Au NP size). For the smallest Au NPs, the shift was smaller than expected for the 3e process but larger than expected for a 1e oxidation. While the shifts are not exactly as expected on the basis of the reported $E°$ values, the fact that a shift occurs strongly suggests that the peaks are due to oxidation of Au in the presence of halides, which was an important conclusion in order to confirm the dramatic negative shift in oxidation potential with decreasing NP size. If we assume that the different-sized NPs oxidize by the same

dx.doi.org/10.1021/ja2108933 | J. Am. Chem. Soc. 2012, 134, 5014−5017

process, then the difference in oxidation of Au in the presence of Br^- and Cl^- depends on the size of the Au, since the shifts in the potential are very different with decreasing Au NP size. This unexpected result is the first report of size-dependent reactivity between Au and halides.

Figures 1 and 2 show convincing evidence of a dramatic negative shift in oxidation potential for small <4 nm diameter Au NPs in the presence of halides, but the peaks in the low-potential region were relatively small. To increase the peak current (or charge) associated with smaller NPs, we synthesized Au NPs by borohydride reduction of $AuCl_4^-$ in the presence of citrate, stopping the reaction after 15 min instead of the normal 2 h, with the hope of capturing smaller Au NPs at an earlier stage of the nucleation and growth process. Figure 3A (blue

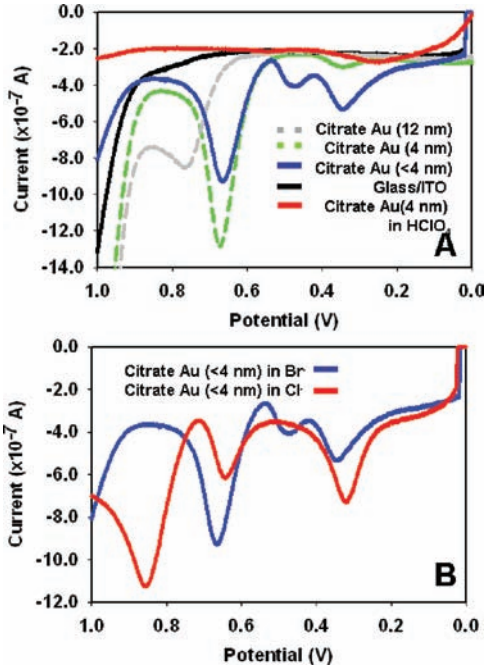

Figure 3. (A) LSVs of citrate-coated Au NPs with diameters of 12, 4, and <4 nm in 0.1 M $HClO_4$ + 0.01 M KBr. The samples with glass/ITO only and 4 nm diameter citrate-coated Au NPs in $HClO_4$ only are shown for comparison. (B) LSVs of citrate-coated <4 nm diameter Au NPs in Br^- solution (blue plot) and Cl^- solution (red plot).

plot) shows the LSV obtained in 0.01 M KBr + 0.1 M $HClO_4$ for the Au NPs synthesized for 15 min and attached to amine-functionalized glass/ITO. The LSV exhibits two oxidation peaks in the low-potential region (300−500 mV) with a much larger intensity relative to the higher-potential oxidation peak near 670 mV. In comparison, the LSV for the 4 nm average diameter Au NPs prepared by reduction for 2 h (green plot) shows only one very small oxidation peak in the low-potential region and a relatively larger peak near 675 mV. The LSV for the larger 12 nm average diameter Au NPs (gray plot) exhibits one main peak near 780 mV with no discernible peaks at the lower potentials. Figure 3A also shows LSVs for the amine-functionalized glass/ITO electrode with no Au NPs (black plot) in KBr + $HClO_4$ and for amine-functionalized glass/ITO coated with 15 min Au NPs in $HClO_4$ only (red plot), which demonstrate that these peaks are not present in the background or for Au NPs without Br^- present. On the basis of the absence of these peaks for larger Au NPs and the control experiments, we attribute the peaks at lower potentials to the oxidation of <4 nm diameter Au NPs, confirming that reduction for 15 min successfully allowed the isolation and measurement of a larger population of <4 nm diameter Au NPs.

Figure 3B compares the LSVs of amine-functionalized glass/ITO electrodes coated with the 15 min-synthesized Au NPs in solutions containing Cl^- and Br^-. The results for three different samples (Figures S3 and S4) showed that the peak potentials were highly reproducible while the peak current (or charge) varied because of differences in NP coverage on the electrode. The same three peaks appeared in both sets of LSVs but were again shifted in the positive direction for Cl^- relative to Br^-. The shifts decreased with decreasing oxidation potential, with values of 190 and 160 mV for peaks III and II, respectively, while the lowest oxidation peak (peak I) near 300 mV was actually ∼30 mV more negative for Cl^- than for Br^-. The halide-dependent oxidation potentials strongly suggest that the peaks are due to halide-assisted Au oxidation, and the LSVs clearly show a dramatic negative shift for <4 nm diameter Au NPs. The oxidation potential of the very smallest population of Au NPs again appeared to be less sensitive to the halide present. Further experiments are needed to better understand this interesting phenomenon.

Figure S5 shows UV−vis absorption spectra of Au NPs reduced for 15 and 120 min. The localized surface plasmon band for Au near 530 nm was more pronounced for the Au NPs reduced for 120 min, which is consistent with the larger average diameter of 4.1 ± 0.7 nm for the 120 min sample relative to the value of 2.3 ± 0.5 nm for the 15 min sample, as measured by TEM (Figure S6).

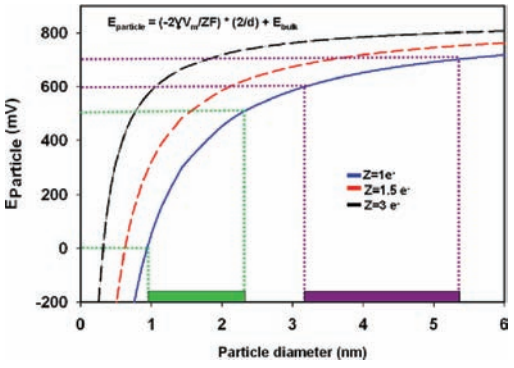

Figure 4. Theoretical shift in the oxidation potential as a function of Au NP diameter from 0 to 6 nm based on the Plieth equation. The green and violet dashed lines respectively represent the lower and higher oxidation potentials observed in Figures 1−3.

Figure 4 shows a plot of the peak oxidation potential for the Au NPs ($E_{particle}$) as a function of the diameter from 0 to 6 nm, based on the Plieth equation:[4]

$$E_{particle} = \left(-\frac{2\gamma V_m}{ZF}\right)\left(\frac{2}{d}\right) + E_{bulk} \quad (1)$$

where E_{bulk} is the oxidation potential of the bulk metal (taken as 850 mV on the basis of the oxidation of ∼50 nm diameter Au NPs under our conditions), γ is the surface tension (1880 erg cm^{-2}),[4] V_m is the molar volume (10.21 cm^3 mol^{-1}),[4] Z is the number of electrons, F is Faraday's constant, and d is the NP diameter. It should be noted that surface stress, instead of surface tension, is more appropriate for the calculation, so the

dx.doi.org/10.1021/ja2108933 | J. Am. Chem. Soc. 2012, 134, 5014−5017

use of γ could be a potential source of error.[5] Three plots are shown with different values of Z, since we previously showed that the oxidation on average involves 1.5 electrons.[12b] Others determined an average of 1.9 electrons[14] or used one electron[11b] in the analysis of Au NP oxidation in the presence of halides. The dashed lines in the plot show the potential ranges where we observed oxidation peaks in Figures 1−3. The low-potential region (0−500 mV), corresponding to 1.0 to ∼2.3 nm diameter Au NPs according to eq 1, is highlighted in green. The higher-potential region (600−700 mV), corresponding to ∼3−5 nm diameter Au NPs, is highlighted in violet. The ranges would be slightly different yet still reasonable for Z = 1.5, but the plot for Z = 3 would not fit our data. Given the uncertainty in the surface stress, we believe the data fit reasonably well for a 1e or 1.5e process.

It is important to make a rough comparison of the TEM data and the electrochemical data in these studies. For example, the charge under the high-potential oxidation peak for Au MPCs is 50 times larger than the cumulative charge of the low-potential oxidation peaks. Taking into account the fact that a 4 nm diameter Au NP contains ∼2400 atoms, as compared with ∼300 atoms for a 2 nm diameter Au NP,[15] that would correspond to ∼86% of the 4.0 nm Au NPs versus 14% of the 2.0 nm Au NPs on the electrode surface. If we roughly consider ≥3.0 nm Au NPs as 4.0 nm NPs and ≤2.9 nm Au NPs as 2.0 nm NPs, the TEM based percentages for these populations would be 29% and 71%, respectively. The electrochemical and TEM data are therefore not in good agreement. For the same analysis with the 15 min citrate-coated Au NPs, the LSV-determined values are 24% and 76%, compared with the TEM-based values of 14% and 86% for ≥3.0 nm and ≤2.9 nm Au NPs, respectively. This is much better agreement. For the Au MPCs, we believe the larger value for the LSV data relative to the TEM data is due to a greater propensity for large Au MPCs to adsorb to the electrode surface because of their lower solubility in the toluene solution and the longer time period used for adsorption (≥2 days). Aggregation or the electrochemical desorption and ozone treatment could also have resulted in larger NPs on the electrode surface than expected. In the case of the citrate-coated Au NPs, we believe the agreement is better because the attachment is electrostatic and relatively fast (5 min) and there was no other treatment.

The oxidation peak for larger-sized Au NPs appears as one broad peak in Figures 1−3, whereas the population of smaller Au NPs appears as multiple distinct peaks. This is due to the much larger oxidation potential difference for a small change in diameter for Au NPs in the 1−2 nm range. For example, the expected difference in the oxidation potential between 3.0 and 4.0 nm diameter NPs is 66 mV. The difference between 2.0 and 2.4 nm diameter Au NPs is also predicted to be 66 mV and the difference between 1.4 and 2.0 nm diameter NPs is 170 mV. These large differences in oxidation potential with a small difference in Au NP size render them more resolvable by LSV, leading to multiple peaks. In general, it is difficult to make an exact comparison between the TEM and electrochemistry results because of the uncertainties in the TEM-measured diameters at these very small sizes and in the size of the Au NPs actually adsorbed on the electrode surface.

In summary, we have reported a dramatic negative thermodynamic shift in the oxidation potential for <4 nm diameter Au NPs. The oxidation was as large as 850 mV negative of the value for bulk Au for the smallest NPs synthesized. The lowest oxidation potentials observed are consistent with 1−2 nm diameter Au NPs on the basis of the Plieth equation. While the details of the oxidation reactions involved (3e, 1e, and chemical) are not well understood, the data fit best with the Plieth equation for a process involving one or an average of 1.5 electrons. Interestingly, the oxidation of the smallest Au NPs in the presence of Br^- and Cl^- exhibits less dependence on the halide used, which is very different from bulk Au behavior. While more details must be worked out, this study clearly shows the remarkable difference in reactivity and large decrease in stability for small metallic nanostructures.

■ ASSOCIATED CONTENT

Supporting Information

Experimental details; thiol removal process; and LSV, UV−vis, and TEM data. This material is available free of charge via the Internet at http://pubs.acs.org.

■ AUTHOR INFORMATION

Corresponding Author

f.zamborini@louisville.edu

Notes

The authors declare no competing financial interest.

■ ACKNOWLEDGMENTS

We gratefully acknowledge financial support from the National Science Foundation (CHE-0848883). R.A.M. acknowledges research-assistant support from the Department of Energy (EE-00003206) through the Conn Center for Renewable Energy Research. We thank Jacek Jasinski for the TEM analysis.

■ REFERENCES

(1) Shang, L.; Dong, S.; Nienhaus, G. U. *Nano Today* **2011**, *6*, 401.
(2) (a) Radniecki, T. S.; Stankus, D. P.; Neigh, A.; Nason, J. A.; Semprini, L. *Chemosphere* **2011**, *85*, 43. (b) Zook, J. M.; Long, S. E.; Cleveland, D.; Geronimo, C. L. A.; MacCuspie, R. I. *Anal. Bioanal. Chem.* **2011**, *401*, 1993.
(3) Henglein, A. *J. Phys. Chem.* **1993**, *97*, 5457.
(4) Plieth, W. J. *J. Phys. Chem.* **1982**, *86*, 3166.
(5) (a) Tang, L.; Han, B.; Persson, K.; Friesen, C.; He, T.; Sieradzki, K.; Ceder, G. *J. Am. Chem. Soc.* **2010**, *132*, 596. (b) Tang, L.; Li, X.; Cammarata, R. C.; Friesen, C.; Sieradzki, K. *J. Am. Chem. Soc.* **2010**, *132*, 11722.
(6) Del Pópolo, M.; Leiva, E.; Klein, H.; Meier, J.; Stimming, U.; Mariscal, M.; Schmickler, W. *Appl. Phys. Lett.* **2002**, *81*, 2635.
(7) Kolb, D. M.; Englemann, G. E.; Ziegler, J. C. *Angew. Chem., Int. Ed.* **2000**, *39*, 1123.
(8) Ng, K. H.; Liu, H.; Penner, R. M. *Langmuir* **2000**, *16*, 4016.
(9) Ward Jones, S. E.; Campbell, F. W.; Baron, R.; Xiao, L.; Compton, R. G. *J. Phys. Chem. C* **2008**, *112*, 17820.
(10) Redmond, P. L.; Hallock, A. J.; Brus, L. E. *Nano Lett.* **2005**, *5*, 131.
(11) (a) Brainina, K. Z.; Galperin, L. G.; Galperin, A. L. *J. Solid State Electrochem.* **2010**, *14*, 981. (b) Brainina, K. Z.; Galperin, L. G.; Vikulova, E. V.; Stozhko, N. Y.; Murzakaev, A. M.; Timoshenkova, O. R.; Kotov, Y. A. *J. Solid State Electrochem.* **2011**, *15*, 1049.
(12) (a) Ivanova, O. S.; Zamborini, F. P. *J. Am. Chem. Soc.* **2010**, *132*, 70. (b) Ivanova, O. S.; Zamborini, F. P. *Anal. Chem.* **2010**, *82*, 5844.
(13) Brust, M.; Walker, M.; Bethell, D.; Schiffrin, D. J.; Whyman, R. *J. Chem. Soc., Chem. Commun.* **1994**, 801.
(14) Zhou, Y.-G.; Rees, N. V.; Pillay, J.; Shikhudo, R.; Vilakazi, S.; Compton, R. G. *Chem. Commun.* **2012**, *48*, 224.
(15) Hostetler, M. J.; Wingate, J. E.; Zhong, C.-J.; Harris, J. E.; Vachet, R. W.; Clark, M. R.; Londono, J. D.; Green, S. J.; Stokes, J. J.; Wignall, G. D.; Glish, G. L.; Porter, M. D.; Evans, N. D.; Murray, R. W. *Langmuir* **1998**, *14*, 17.